

# Reduced graphene oxide/ZnO hybrid structure for high-performance photodetection

S. Darbari · V. Ahmadi · P. Afzali · Y. Abdi · M. Feda

Received: 5 August 2014 / Accepted: 4 December 2014 / Published online: 10 December 2014  
© Springer Science+Business Media Dordrecht 2014

**Abstract** We report the optoelectronic behavior of a novel reduced graphene oxide (rGO)/ZnO structure which has been realized by photocatalytic reduction of chemically exfoliated GO sheets. Lateral ZnO nanowires, which are grown between interdigital electrodes by a novel plasma-assisted procedure, are utilized as the photocatalyst metal oxide in the presented heterostructure. Raman spectroscopy and FTIR analyses are utilized to show that photocatalytic reduction of GO sheets, with few (less than 5) layers, occurs after about 30 min of UV-illumination. Low-temperature electrical characterizations are applied to demonstrate one-dimensional behavior of the realized rGO ribbons, with an estimated width of around 30 nm. The optoelectronic characteristics of the fabricated rGO/ZnO hybrid structure also lead to high responsivity of about 12 A/W and a sensitivity of about  $5 \times 10^4$  % (at the bias voltage of  $-5$  V), which entitles the fabricated structure as an efficient photodetector. All in all, our experimental results open up a promising simple approach to fabricate GNR-based devices by assisting lateral ZnO nanowire, without involving nanolithography issues.

**Keywords** Photocatalyst · Reduced graphene oxide · ZnO nanowires · Optoelectronic characteristics

## Introduction

Chemical exfoliation of graphite by powerful oxidizing agents has emerged as a viable route to prepare graphene single sheets. Reduction of graphene oxide restores its electrical characteristics greatly; however, high temperature and harmful chemicals are among the limitations of typical reduction approaches (Schmidt 2001). Thus, it is of a great interest to find low-temperature, safe, bio-compatible alternative reduction methods to prepare graphene or graphene nanostructures. In this regard, different methods have already been proposed including catalytic and photocatalytic processes (Akhavan 2011). One of the graphene research goals is to introduce an energy band gap through fabrication of graphene nanoribbons (GNR). The most straight forward method to produce GNRs is through e-beam lithography; however, such an approach is limited by poor scale resolution, large edge roughness, low throughput, and high costs (Han et al. 2007). Other approaches have been also reported to produce GNRs including unzipping of CNTs (Jiao et al. 2009), and nanoscale thermal reduction of graphene oxide sheets (Wei et al. 2010). Regarding photocatalytic patterning of graphene, Zhang et al. applied TiO<sub>2</sub> photomask for photochemical tailoring

S. Darbari · V. Ahmadi (✉) · M. Feda  
Department of Electrical and Computer Engineering,  
Tarbiat Modares University, Tehran, Iran  
e-mail: v\_ahmadi@modares.ac.ir

P. Afzali · Y. Abdi  
Department of Physics, University of Tehran, Tehran, Iran

of graphene (Zhang et al. 2011) and Akhavan utilized ZnO nano-rods to realize graphene nano-mesh structures by photocatalytic reduction of graphene oxide sheets (Akhavan et al. 2010). In this line of research, we have recently reported the photocatalytic reduction of graphene oxide (GO) in the presence of laterally grown ZnO nanowires to achieve rGO/ZnO heterostructures (Darbari et al. 2013). The presented approach is not limited by high temperature or nanolithography expenses and does not involve any harsh procedure which may lead to boundary defects/roughness, like tearing or etching. Here, we have pursued the related material study and fully investigated the electrical and optoelectronic properties of the achieved structure. Also, we have studied the low-temperature electrical characteristics of the fabricated device and demonstrated that the photocatalytic reduction of GO/lateral ZnO nanowire can lead to realize one-dimensional rGO structures. Then, we applied this approach to fabricate a photodetector (PD) which shows high sensitivity beside a significant enhancement in responsivity, and proposed a mechanism to explain the achieved enhanced optoelectronic performance.

## Fabrication process

Figure 1 indicates the fabrication process schematically, the process which was described in our previous work with details (Darbari et al. 2013). A 100-nm thermal oxide is grown on (100) Si wafer to isolate the structure from the substrate. Then, a 500-nm Zn layer is deposited (Fig. 1a) and patterned to the interdigital-shaped electrodes with a spacing of 10  $\mu\text{m}$  (Fig. 1b). Zn will serve as the growth seed, at the next stage, so that nanowires grow exclusively on the interdigital pre-patterned electrodes. Sample is then placed in a plasma-enhanced chemical vapor deposition (PECVD) chamber to grow lateral ZnO nanowires. ZnO nanowires will be utilized as the photocatalytic metal oxide semiconductor to reduce the GO sheets. For this purpose, sample is first annealed at the temperature of 350  $^{\circ}\text{C}$  for about half an hour, at a base pressure of  $10^{-3}$  Torr. Then oxygen is introduced to the chamber with 100 sccm flow rate, and the sample is exposed to oxygen plasma with a power density of 7  $\text{W}/\text{cm}^2$  subsequently. The substrate temperature is set at 350  $^{\circ}\text{C}$ , and the base pressure is 7 Torr during this step. The appropriate time

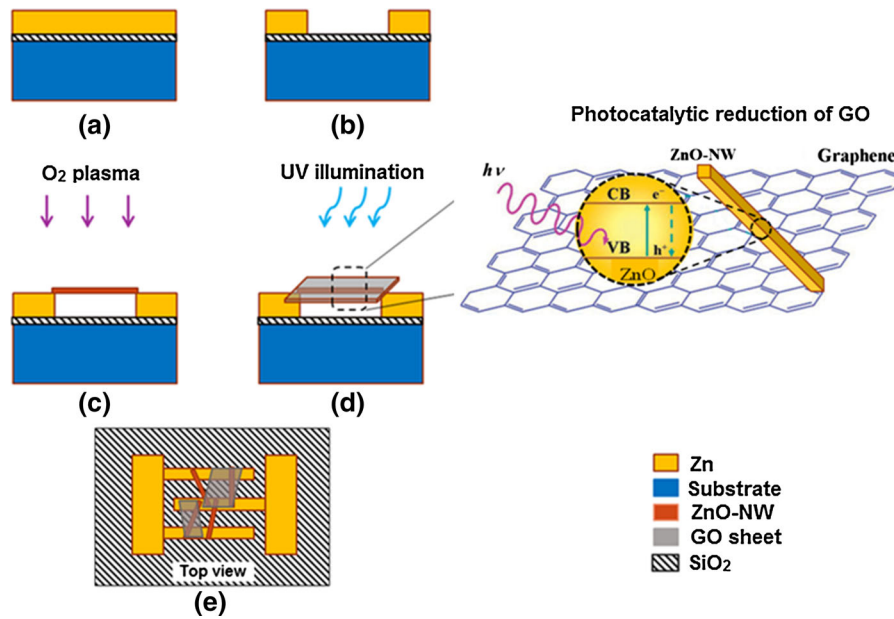
duration of this step is achieved at about 40 min, so that ZnO nanowires grow long enough to reach the neighboring electrode and provide an interconnection (Fig. 1c).

Now, graphite powder is chemically exfoliated to prepare GO suspension through Hummers' method (Hummers 1958). Then GO sheets are dispersed on the base of lateral ZnO nanowires by dip-coating, as shown in Fig. 1d. ZnO nanowires are assisted for photocatalytic reduction of the GO sheets, along the nanowire/GO interface (Fig. 1d). It should be noted here that oxygen groups, which can remain partially after photocatalytic process, can behave as a p-type dopant and result in lightly doped rGO structures (Lv and Terrones 2012). At this stage, a mercury lamp with a maximum radiation wavelength of 365 nm and a power density of 100  $\text{mW}/\text{cm}^2$  is used as the UV source, for photocatalytic reduction. The top view of the prepared sample is depicted schematically in Fig. 1e.

## Results and discussion

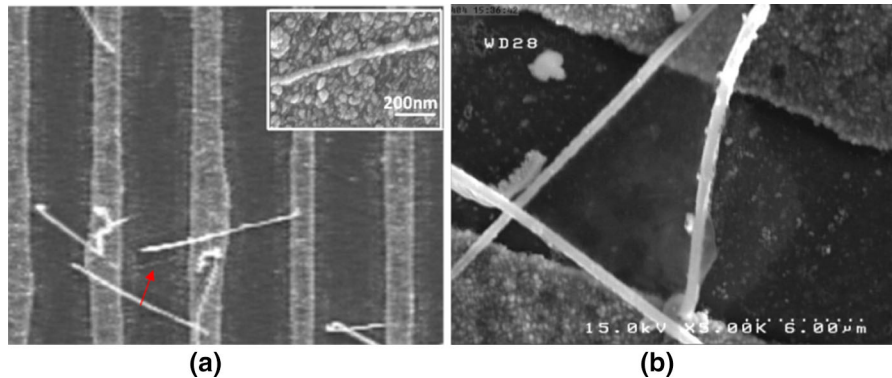
Figure 2a displays the GO sheets dispersed on the interdigital electrodes. Arrow in this figure indicates a nanowire with a thickness below 100 nm which is highlighted in the inset. Figure 2b illustrates a GO sheet suspended on two neighboring ZnO nanowires.

Figure 3 illustrates the Raman spectrum of the realized rGO/ZnO structures, achieved by photocatalytic reduction. This plot shows three individual peaks called D, G, and 2D bands at 1,319, 1,580, and 2,620  $\text{cm}^{-1}$ , respectively. The G band corresponds to  $\text{sp}^2$  carbon-type structures within the rGO sheets, while the D band refers to the structural imperfections in the hexagonal graphitic layers induced by the attachment of hydroxyl or epoxide groups. Thus, lower (higher)  $I_{\text{D}}/I_{\text{G}}$  can be assigned to lower (higher) defects and disorders of the graphitized structures, or equally lower (higher) fraction of  $\text{sp}^3/\text{sp}^2$ -bonded carbon (Tuinstra and Koenig 1970; Ferrari et al. 2000; Graf 2007). The inset displays the  $I_{\text{D}}/I_{\text{G}}$  value as a consequence of UV-irradiation time. Here, it can be observed that more irradiation time decreases the  $I_{\text{D}}/I_{\text{G}}$  value, which is attributed to the progress of photocatalytic reduction of GO sheets. However, irradiation times greater than around 30 min do not lead to higher reduction level and it seems that the reduction progress



**Fig. 1** Schematic of the fabrication process. **a** Zn layer deposited on the thermal oxide layer; **b** patterning Zn layer to achieve interdigital electrodes; **c** growing lateral ZnO nanowires

between neighboring electrodes, by PECVD; **d** dispersing GO sheets and UV-illumination to achieve photocatalytic reduction; **e** top view of the final prepared specimen



**Fig. 2 a** Deposited GO sheets on the ZnO nanowires grown on the pre-patterned interdigital electrodes. *Inset* displays a higher magnification of the highlighted nanowire with a diameter

below 100 nm. **b** The magnified view of a GO sheet suspended between two ZnO nanowires

saturates. Figure 3b magnifies the 2D band in the Raman spectrum of the synthesized rGO sheets. It has been previously shown that few (less than 5) layers of graphene have a broader 2D band (consisting of four individual peaks) in comparison with graphene (Ferrari et al. 2006). Also, increasing of the number of layers more than 5 leads to a significant decrease of the relative intensity of the lower frequency 2D<sub>1</sub> peak. Concerning these points, the observed 2D band is attributed to few layers of reduced graphene.

To further study the chemical bonds, during photocatalytic reduction of GO sheets, FTIR analysis has been utilized. Figure 4 depicts the achieved FTIR spectra for the synthesized GO (red spectrum) and rGO (blue spectrum) sheets.

The achieved spectra for both GO and rGO sheets show oxygen trace in stretching vibrations from C–O, C–OH, and O–H bonds at about 1,060, 1,220, and 3,400 cm<sup>-1</sup>, respectively (Li et al. 2008; Naebe et al. 2014; Choi et al. 2010; Ban et al. 2012). It can be

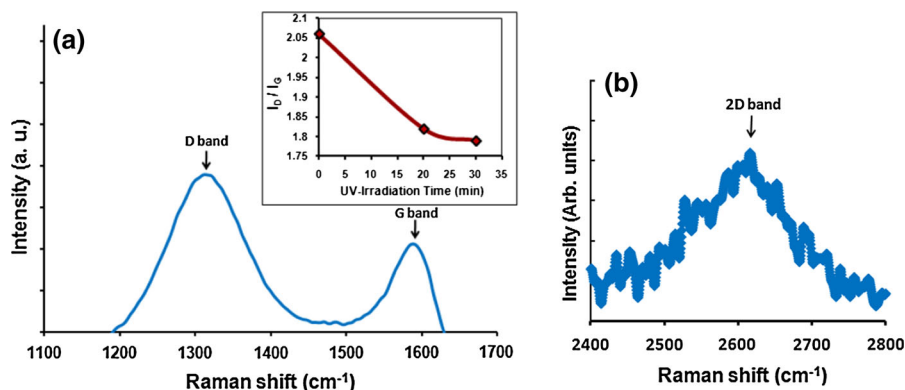


**Fig. 3** Raman spectrum of the synthesized rGO sheets; **a** D and G bands at about  $1,319$  and  $1,580$   $\text{cm}^{-1}$ , respectively, and **b** the magnified 2D band at  $2,620$   $\text{cm}^{-1}$ , as the fingerprints of rGO

sheets. *Inset* in part (a) shows that  $I_D/I_G$  value decreases as a consequence of UV-irradiation time and reaches a steady state after about 30 min of irradiation

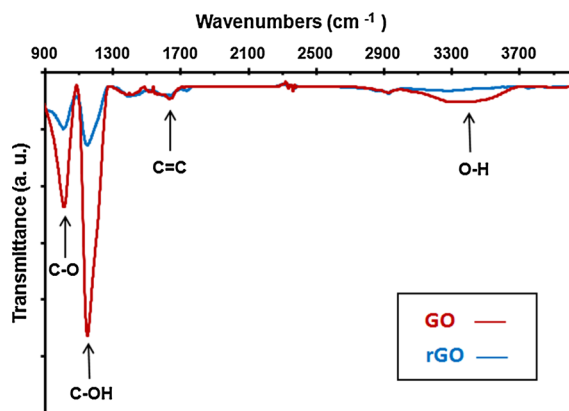


**Fig. 4** FTIR spectra corresponding to the synthesized GO (*red*) and rGO (*blue*) sheets. A significant reduction can be observed in the concentration of oxygen groups after photocatalytic reduction. (Color figure online)

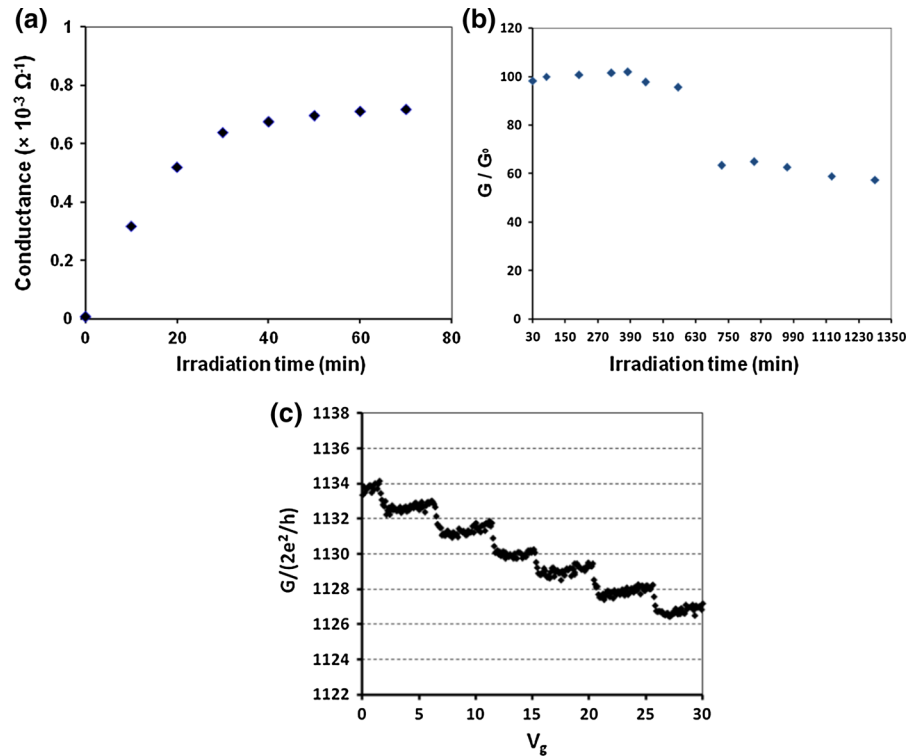
observed by FTIR spectroscopy that oxygen groups are significantly reduced due to deoxygenation in rGO, while the trace of C=C bonds (at  $1,620$   $\text{cm}^{-1}$ ) are approximately the same in both spectra.

To investigate the effect of photocatalytic reduction on the electrical behavior of the fabricated structure, we measure the electrical conductance of the device at different stages. For this purpose, we monitor the conductance of the fabricated structure (the conductivity between two interdigital electrodes of Fig. 1e), as the photocatalytic process progresses. Figure 5a displays the variation of the conductivity versus UV-irradiation time, at room temperature. It can be observed that conductivity increases significantly by

photocatalytic reduction of GO sheets and saturates after about 30 min of UV-illumination. The observed increasing and then saturating behavior of the conductivity during UV-illumination is in agreement with the achieved Raman spectrum (inset of Fig. 3a); and are both attributed to a significant increment of the graphitized  $\text{sp}^2$  structures over the disorders. The conductivity enhancement ( $G/G_0$ ) is measured about  $100 \pm 11$ . The tolerance is related to the variation of structural parameters in different samples. The observed significant conductivity enhancement implies that the conductivity of the prepared rGO region is significantly higher than ZnO nanowires or un-reduced GO zone. As a result, the rGO region can be considered as the equivalent conductive path between interdigital electrodes. It is also worth mentioning that we can assume the photocatalytic reduction completed after about 30 min of UV-irradiation. Hence, we have applied the samples with 30 min of illumination for the proceeding electrical and optoelectrical investigations.

To evaluate the efficiency of the photocatalytic reduction, we have compared our electrical result with another report which took advantage of thermal reduction. For instance, Wei et al. reported a tunable local reduction of GO sheets by a hot scanning AFM probe. They achieved  $G/G_0$  values of around 600 and 10, for hot probes with temperatures of around  $1,200$  and  $600$   $^{\circ}\text{C}$ , respectively (Wei et al. 2010). It is notable that the observed 100-fold conductivity enhancement is obtained by a simple room-temperature fabrication process, in this paper.

**Fig. 5** **a** Variation of the electrical conductance versus the UV-irradiation time, as a consequence of photocatalytic reduction of GO sheets in the GO/ZnO heterostructure. **b** Long-time variations of the relative conductivity of a completely reduced rGO/ZnO structure. Photodegradation of rGO/ZnO structure leads to conductivity decrement, after about 700 h of UV-irradiation. Measurements in parts (a) and (b) are carried out at room temperature. **c** The measured conductance quantization of the synthesized GNRs, at a temperature of about 80 K



Photodegradation of rGO sheets, in the vicinity of ZnO nanostructures, is another concern that must be considered in the proposed structure. Akhavan and colleagues showed that when UV is irradiated on the  $TiO_2/GO$  structures, a rapid photocatalytic reduction of GO sheets occurs first; and carbon content of the rGO sheets decreases gradually after long irradiation times (Akhavan et al. 2010). Regarding this, we have investigated the photodegradation of the realized rGO/ZnO heterostructure by monitoring variations of the relative electrical conductivity ( $G/G_0$ ), during about 20 h of UV-irradiation (Fig. 5b). It should be noted that the investigated sample has been initially irradiated for about 30 min to realize the rGO/ZnO structure. Figure 5b illustrates that the conductivity of the realized rGO drops down to about 60 % after around 700 min of UV-irradiation and then decreases gradually, which can be related to photodegradation of the carbon contents in rGO sheets.

Note that the realized rGO structure, which is realized at the GO/ZnO nanowire interface, is embedded inside the GO sheet. Also, considering the significant band gap difference between rGO and GO, we can assume a lateral confinement for electrons

inside rGO region (Wei et al. 2010). Due to the narrow width of a ZnO nanowire/GO intersection in comparison to the related length, we expect to observe one-dimensional behavior for the achieved rGO structure. In this regard, we study the electrical conductance of the synthesized rGO structure at low temperature, to observe the subband formation. For this purpose, we apply a gate voltage to the underlying substrate and investigate the electrical conductance of the rGO structure while sweeping the gate voltage. It should be noted that this measurement is carried out at a temperature of about 80 K. Figure 5c shows the achieved conductance plateau features. Simulation results based on the Landauer approach have shown that if quantization energy ( $\Delta E$ ) of the GNR is higher than 6 kT, the conductance quantization can be appeared in the measurements (Lin et al. 2008). Hence, a minimum energy quantization ( $\Delta E$ ) of about 40 meV can be deduced from the clearly observable conductance plateau of our synthesized rGO structure, at 80 K (Fig. 5c). According to these simulations, band gap can be estimated by  $E_g = 2\alpha \cdot \Delta E$ , with  $\alpha \approx 0.4$ . Also, it is well established from both experimental and theoretical articles that the ribbon

width is inversely related to the band gap of graphene nanoribbon (Han et al. 2007). Thus, a band gap of about 32 meV and a ribbon width below 30 nm can be estimated for the synthesized rGO structure.

In this line of research, we monitored the current–voltage characteristic of the fabricated rGO/ZnO nanowire device, as shown in Fig. 6. This measurement is carried out, both at 80 K and at room temperature (RT). It should be noted that no gate bias

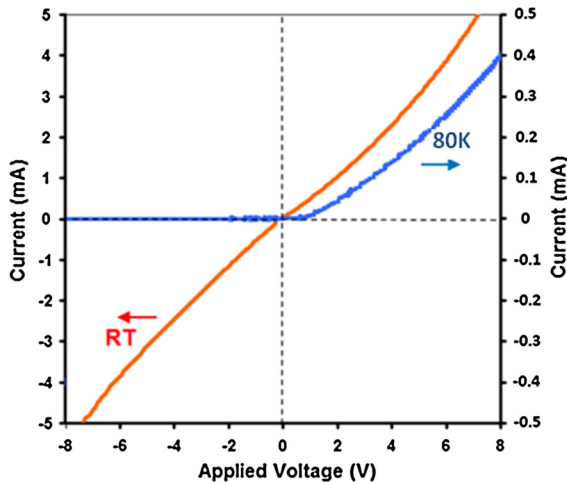


**Fig. 6** I–V characteristics of the fabricated sample measured at about 80 K (*blue curve*) and at RT (*red curve*). (Color figure online)

has been applied at this stage. Blue curve ( $\approx 80$  K) shows a rectifying electrical behavior, while red curve (RT) shows an almost linear behavior in Fig. 6. We believe that the narrow band gap of the synthesized rGO structure leads to a metal–semiconductor and a Schottky contact behavior, at low temperatures. Since the thermal energy of the carriers is comparable with the rGO band gap, the semiconducting behavior diminishes at room temperature and a semi-metallic behavior emerges. This hypothesis results in a nearly linear and symmetric characteristic (red curve), as shown in Fig. 6. Also, higher thermal generation leads to higher carrier density and current level for the red curve, as compared to the blue curve.

As shown in Fig. 6, the fabricated rGO-based device shows a diode-like behavior at low temperatures. Thus, we investigate the optoelectronic characteristics of the fabricated rGO/ZnO nanowire-based PD. It should be noted again that the prepared sample is irradiated and investigated, at a temperature of about 80 K. Parts (a) and (b) of Fig. 7 illustrate the optoelectric characteristics of the fabricated PD, in forward- and reverse-bias regions.

It is observable that both red and green sources raise the photocurrent, while the effect of red irradiation is found to be more pronounced. Also, the induced photocurrent is considerable in both reverse- and forward-bias regimes, which shows the high

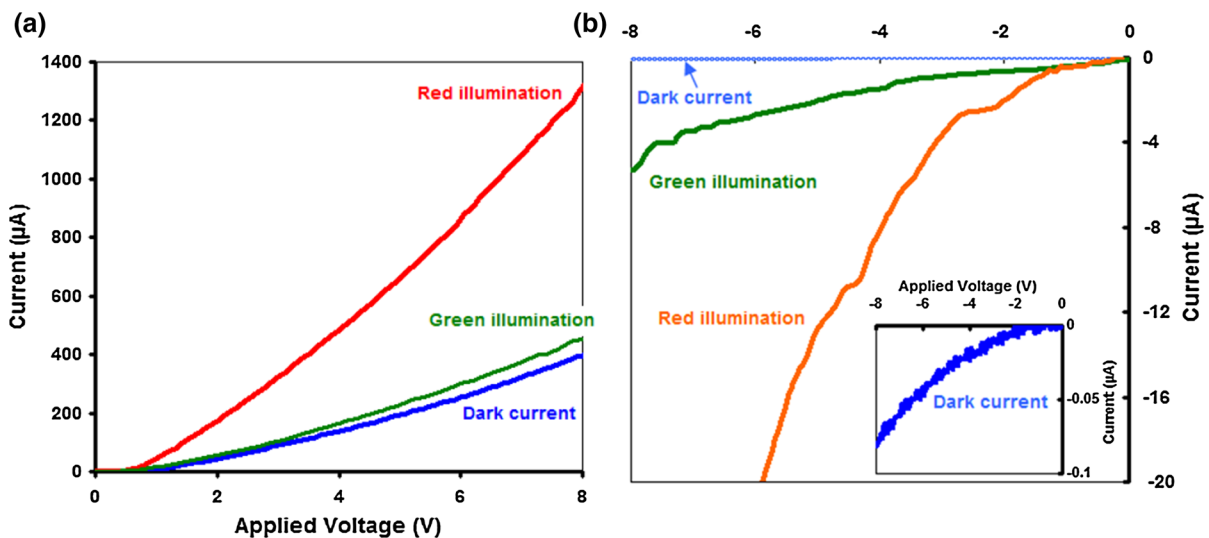


**Fig. 7** Effect of red and green laser irradiation on the I–V characteristic of the fabricated GNR-based device at **a** forward- and **b** reverse-bias regions. The *Inset* highlights the dark current

versus the applied voltage of the photodiode. The measurements are carried out at LNT

sensitivity of the fabricated PD. Figure 7b shows that red light intensifies the dark current up to  $5 \times 10^4 \%$  at a bias voltage of  $-5$  V. Also, the measured sensitivity (sensitivity =  $I_{\text{light}}/I_{\text{dark}}$ ) is about  $8 \times 10^3 \%$  for green irradiation, at the same bias. Parts (a) and (b) of Fig. 8 illustrate the achieved sensitivity and responsivity ( $(I_{\text{light}} - I_{\text{dark}})/P_{\text{illumination}}$ ) versus the applied voltage. Previous reports have demonstrated a maximum responsivity of about  $10^{-2}$  A/W for the graphene-based PDs (Mueller et al. 2010). Here, we achieve a responsivity of around 12 A/W beside a sensitivity of about  $5 \times 10^4 \%$  for the fabricated PD (at the bias voltage of  $-5$  V). Thus, the fabricated GNR-based PD yields about three

orders of magnitude enhancement in responsivity value, in comparison to the typical graphene-based PDs (Mueller et al. 2010).

We believe that the achieved high responsivity can be attributed to the effect of rGO/GO heterostructures. The energy band bending occurred at the vicinity of the heterojunctions can lead to a charge separation and hinders recombination of the photogenerated carriers. Due to the narrow width of the rGO region, this effect can enhance the photocurrent and the output performance significantly. Figure 9a and b displays the investigated structure and the discussed hypothesis schematically. Part (a) in this figure indicates the investigated structure, in which rGO region is

**Fig. 8** Variations of the **a** sensitivity and **b** responsivity of the fabricated GNR-based photodiode versus the applied voltage. High sensitivity and responsivity can be achieved at relatively low voltages

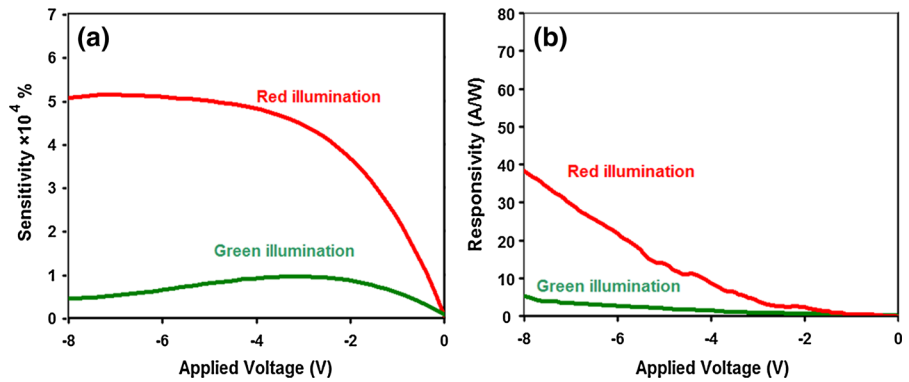
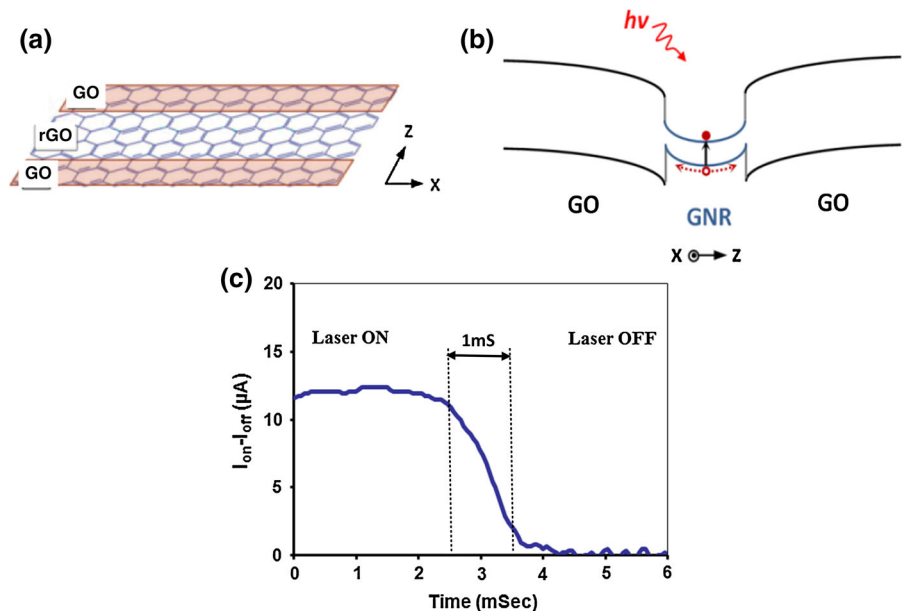


**Fig. 9** **a** The schematic of the synthesized GO/rGO/GO heterostructure. **b** The proposed band diagram and the charge separation process. **c** Temporal response of the fabricated PD. The measured carrier lifetime is around 1 ms



embedded in the GO sheet. Also, Fig. 9b illustrates the simplified band diagram in which the photogenerated holes are drifted to the rGO/GO interfaces, due to the built-in electric field. In this regard, Konstantatos et al. have also reported an ultrahigh responsivity of about  $10^7$  A/W by a hybrid graphene/QD structure (Konstantatos et al. 2012). Similarly, they have attributed this great performance to the charge separation occurring at the graphene/QD heterojunction. To investigate the discussed hypothesis experimentally, we study the time-resolved photocurrent response of the fabricated device as a result of illumination. Figure 9c shows the measured temporal response, which gives the photogenerated carrier's lifetime of about 1 ms. The measured lifetime is significantly enhanced in comparison with the reported PDs based on pristine graphene structures (tens of picoseconds) (Xia et al. 2009). This observation is in agreement with the proposed charge separation assumption in the fabricated graphene-based PD.

Figure 10a shows the response of the fabricated PD to different wavelength irradiations (at a bias of  $-5$  V). It can be seen that higher wavelength results in higher output photocurrent and the output response decays significantly for wavelengths lower than around 500 nm.

To enlighten the role of the synthesized rGO in the observed optoelectric behavior, we investigate the behavior of the pure ZnO nanowire-based device. Figure 10b shows the response of the bare ZnO nanowire-based structure superimposed on the results of the presented rGO-based structure, which have been highlighted by red and blue arrows, respectively. Two previously utilized sources (532 and 635 nm) are applied for this measurement. As expected, the sensitivity of the rGO-based structure is about three orders of magnitude higher than the pure ZnO nanowire-based structure, in response to red and green illumination. Also, it should be noted that the observed low response of the ZnO nanowire-based structure to the visible range irradiation can be attributed to some possible defect-induced trap levels (Sheetz et al. 2009).

The other worthy point about Fig. 10b is the opposite trend of the measured sensitivity for pure ZnO structure and rGO structure. It can be seen in this figure that the bare ZnO nanowire-based device results in higher sensitivity at lower irradiation wavelength; however, rGO-based structure shows an inverse trend.

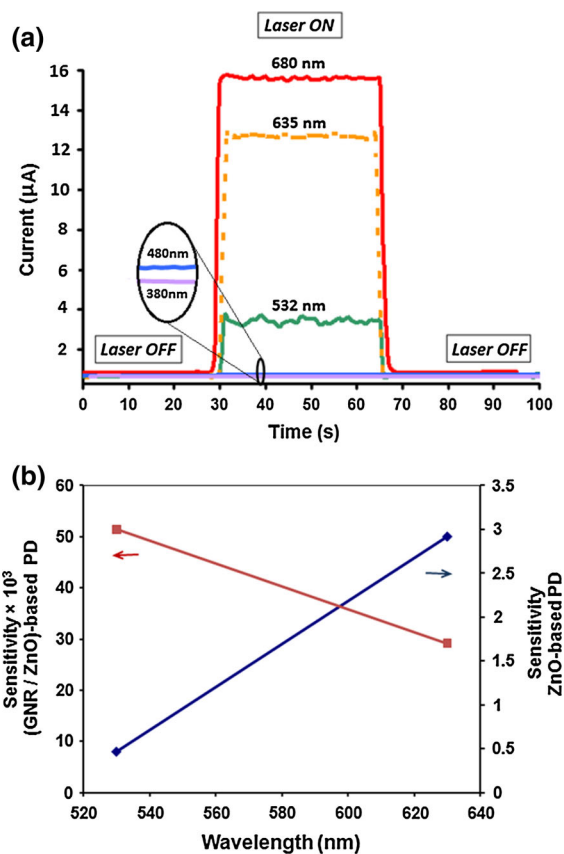


**Fig. 10** **a** The response of the fabricated PD to different wavelength irradiations. A wavelength of around 500 nm can be estimated as the lower limit of the operational wavelength. **b** The achieved sensitivity of the bare ZnO-based structure in comparison with the presented rGO/ZnO-based structure

## Conclusion

We have applied photocatalytic reduction in a GO/ZnO nanowire structure to realize rGO ribbons embedded in GO sheets. Raman spectroscopy and FTIR analysis are utilized to prove the photocatalytic reduction of GO sheets. Electrical characterizations show a 100-fold increment in the conductivity of the reduced GO sheets, after about 30 min of UV-irradiation. The reported approach has been directly utilized to fabricate rGO-based PD which led to a high responsivity of about 12 A/W, and a sensitivity of about  $5 \times 10^4$  % (at the bias voltage of  $-5$  V). The achieved responsivity was enhanced over three orders of magnitude in comparison to previously reported graphene-based PDs, which is attributed to the charge separation of photogenerated carriers at the rGO/GO



interface. All in all, the reported fabrication procedure can be proposed as an environment-friendly, efficient, and simple technique to realize efficient graphene-based devices.

## References

- Akhavan O (2010) Graphene nanomesh by ZnO nanorod photocatalysts. *ACS Nano* 4:4174–4180
- Akhavan O (2011) Photocatalytic reduction of graphene oxides hybridized by ZnO nanoparticles in ethanol. *Carbon* 49:11
- Akhavan O, Abdolahad M, Esfandiari M, Mohatashamifar M (2010) Photodegradation of graphene oxide sheets by TiO<sub>2</sub> nanoparticles after a photocatalytic reduction. *J Phys Chem C* 114:12955–12959
- Ban FY, Majid SR, Huang NM, Lim HN (2012) Graphene oxide and its electrochemical performance. *Int J Electrochem Sci* 7:4345–4351
- Choi EY, Han TH, Hong J, Kim JE, Lee SH, Kimaand HW, Kim SO (2010) Noncovalent functionalization of graphene with end-functional polymers. *J Mater Chem* 20:1907–1912
- Darbari S, Ahmadi V, Afzali P, Abdi Y (2013) Photocatalytic reduction of GO/ZnO to achieve GNRs for optoelectronic applications. *J Phys D* 46:385101
- Ferrari AC, Robertson J (2000) Interpretation of Raman spectra of disordered and amorphous carbon. *Phys Rev B* 61:14095–14107
- Ferrari AC, Meyer JC, Scardaci V, Casiraghi C, Lazzeri M, Mauri F, Piscanec S, Jiang D, Novoselov KS, Roth S, Geim AK (2006) The Raman fingerprint of graphene. *Phys Rev Lett* 97:187401
- Graf D (2007) Spatially resolved Raman spectroscopy of single- and few-layer graphene. *Nano Lett* 7:238–242
- Han MY, Ozyilmaz B, Zhang Y, Kim P (2007) Energy band-gap engineering of graphene nanoribbons. *Phys Rev Lett* 98:206805
- Hummers WOR (1958) Preparation of graphite oxide. *J Am Chem Soc* 80:1339
- Jiao L, Zhang L, Wang X, Diankov G, Dai H (2009) Narrow graphene nanoribbons from carbon nanotubes. *Nature* 458:877
- Konstantatos G, Badioli M, Gaudreau L, Osmond J, Bernechea M, Arquer FPG, Gatti F, Koppens FHL (2012) Hybrid graphene–quantum dot phototransistors with ultrahigh gain. *Nat Nanotechnol* 7:363
- Li D, Muller MB, Gilje S, Kaner RB, Wallace GG (2008) Processable aqueous dispersions of graphene nanosheets. *Nat Nanotechnol* 3(2):101–105
- Lin YM, Perebeinos V, Chen Z, Avouris P (2008) Electrical observation of subband formation in graphene nanoribbons. *Phys Rev B* 78:161409
- Lv R, Terrones M (2012) Towards new graphene materials: doped graphene sheets and nanoribbons. *Mater Lett* 78:209–218
- Mueller T, Xia F, Avouris P (2010) Graphene photodetectors for high-speed optical communications. *Nat Photonics* 4:297
- Naebe M, Wang J, Amini A, Khayyam H, Hameed N, Li LH, Chen Y, Fox B (2014) Mechanical property and structure of covalent functionalized graphene/epoxy nanocomposites. *Sci Rep* 4:4375
- Schmidt W (2001) Hydrazine and its derivatives, preparation, properties, applications, 2nd edn. Wiley, New York
- Sheetz RM, Ponomareva I, Richter E, Andriotis AN, Menon M (2009) Defect-induced optical absorption in the visible range in ZnO nanowires. *Phys Rev B* 80:195314
- Tuinstra F, Koenig JL (1970) Raman spectrum of graphite. *J Chem Phys* 53:1126–1130
- Wei Z, Wang D, Kim S, Kim SY, Hu Y, Yakes MK, Laracuente AR, Dai Z, Marder SR, Berger C, King WP, Heer WA, Sheehan PE, Riedo E (2010) Nanoscale tunable reduction of graphene oxide for graphene electronics. *Science* 328:1373
- Xia F, Mueller T, Lin Y, Valdes-Garcia A, Avouris P (2009) Ultrafast graphene photodetector. *Nat Nanotechnol* 4:839
- Zhang L, Diao S, Nie Y, Yan K, Liu N, Dai B, Xie Q, Reina A, Kong J, Liu Z (2011) Photocatalytic patterning and modification of graphene. *J Am Chem Soc* 133:2706